Proceedings of the ASME 2015 International Design Engineering Technical Conferences & Computers and Information in Engineering Conference
IDETC/CIE 2015
August 2-5, 2015, Boston, Massachusetts, USA

DETC2015-47749

DRAFT: ANALYSIS AND DESIGN OF A REMOTE CENTER COMPLIANCE UNIVERSAL JOINT

Pierre-Olivier Dubois
Robotic laboratory
Department of Mechanical Engineering
Polytechnique Montreal
Montreal, Quebec, H3T 1J4
Email: pierre-olivier.dubois@polymtl.ca

Lionel Birglen
Robotic laboratory
Department of Mechanical Engineering
Polytechnique Montreal
Montreal, Quebec, H3T 1J4
Email: lionel.birglen@polymtl.ca

ABSTRACT

This paper presents a novel mechanical design of a lower mobility remote center compliance linkage. This mechanism consists in three platforms connected by three legs with universal joints. Two of these platforms are attached to the ground while last one is the mobile platform. Using screw theory, it is first demonstrated that this mechanism allows its mobile platform to rotate around a fixed point in space without having a joint directly connected to this point. Indeed, knowing the mobility of the two former platforms, it is possible to define a wrench system for each leg and thus, find the reciprocal twist system of the mobile platform. Then, the results of the optimization of the mechanism's design through a genetic algorithm is presented using the conditioning of its Jacobian Matrix as a criterion. Finally, a compliant version of the mechanism is developed and a finite element analysis (FEA) simulation demonstrates the proper mobility of the system under typical loading scenarios.

NOMENCLATURE

DOF	Degrees of Freedom
$\mathbf{A}$	Matrix (bold uppercase)
$\mathbf{a}$	Vector (bold lowercase)
A, a	Scalar
C_i	$\cos(\theta_i)$
S_i	$\sin(\theta_i)$
C_{ij}	$\cos(\theta_i + \theta_j)$
S_{ij}	$\sin(\theta_i + \theta_j)$
$\$$	Screw
ξ	Twist (kinematic screw)
ζ	Wrench (force/torque screw)
$\mathscr{S}$	Screw System
$\mathscr{V}$	Twist System
$\mathscr{T}$	Wrench System
$\$\circ$	Reciprocal Product Operator
$\$_\mathbf{1} \circ \$_\mathbf{2}$	Reciprocal Product of $\$_\mathbf{1}$ and $\$_\mathbf{2}$
$\mathscr{S}^\perp$	Reciprocal System

INTRODUCTION

Textile fabric handling is a daunting but still inevitable task the carbon fiber reinforced plastics (*CFRP*) manufacturing. Indeed, it is the first step of almost every *CFRP* fabrication process. As the demand in *CFRP* has massively increased during the two last decades [1] especially because of an increasing demand from the aerospace industry, automation of this part of the fabrication process has attracted attention. The difficulty of this task however is that it must be done with a tremendous care and precision. Indeed, it has been shown that only a few damaged fibers could lead to important performance degradation. In fact, mathematical models were developed and experimentally validated that demonstrated that only 10 broken fibers out of thousands can produce a stress concentration factor of about 1.5 [2, 3]. Therefore, the design of a gentle textile fabric manipulation system is a critical aspect in the composite industry.

Several papers [1, 4–9] were published about the design of such end-effectors to be attached to an industrial robot but some problems are still not yet solved, for instance the surface adaptation of the gripper remains challenging. Usually, handling end-effectors are designed for a defined geometry (planar or 3D), and do not require shape adaptation. However, this type of designs requires to be changed for every different parts to be handled. This problem can be partly solved by adding mobilities to the gripper. For example, in [7] a solution to this problem was presented where the fabric gripper was installed on a revolute joint and stabilized using springs. However, this solution is still not optimal for all uses. Indeed, it is limiting the adaptation to only one *DOF*. With the aim of creating an improved shape adaptive fabric handling end-effector, the design of a mechanism allowing the fabric gripper to have two *DOF* (namely a rotation around two axis) is primordial. The desired motion is presented in Figure 1.

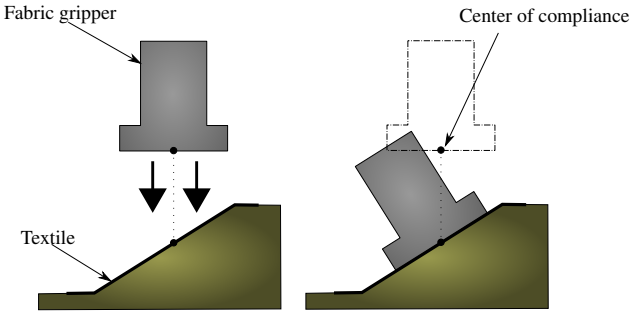

FIGURE 1. DESIRED MOTION

Various types of grippers exist for textile manipulation, each one having their own advantages and drawbacks. Many papers in the literature [10–13] already presented these in details. The one used for this paper was chosen in order to minimize the impact of the grasp on the material as it can be very detrimental. Specifically, the gripper targeted to be used is a *Schamlz Composite Gripper SCG*. This gripper use the Coanda effect to generate a vacuum between the textile and the surface of the gripper, which minimize damage to the fibers.

As the main idea is then to add mobilities between the robot's wrist and the *SCG*, the solution is to use a remote center compliance (*RCC*) mechanism. *RCC*s have been used since the mid 70's [14–16] to provide additional *DOF* to an end-effector. It is most commonly used for "peg-in-hole" assembly [17, 18] in which an object is inserted inside a hole while allowing a certain incertitude in the position and orientation between both of the latter. Other uses also include self-centering and avoidance of wedging or jamming [19].

The novel *RCC* designed in this paper is an assembly of three platforms linked by three legs as shown in Figure 2. Platforms A and B are attached to the ground with universal joints (*U-joint*) as well as linked to the legs another set of *U-joints*. The last platform (C) is the mobile part of the mechanism and is only linked to the legs again (with *U-joint*).

MECHANISM ANALYSIS

Approach and Assumptions

In order to analyze the mechanism, it is possible to divide it into three platforms (A, B and C) and three legs (1, 2 and 3) as presented in Figure 2. The analysis will then be divided in four main steps:

1. Computation of the mobility of platforms A and B
2. Computation of the mobility of platform C
3. Actuation / passive element locations
4. Velocity relationship

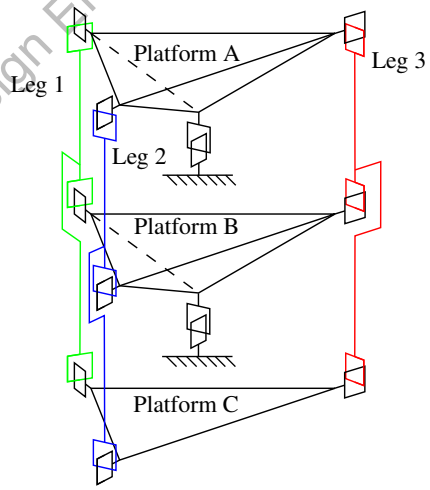

FIGURE 2. KINEMATIC OF THE MECHANISM

Let us first define the twist and wrench systems of a *U-joint*. In Figure 3, the geometrical parameters that will be used in this paper for the kinematic of a *U-joint* are presented. Note that the $(\mathbf{x},\mathbf{y},\mathbf{z})$ axis system revolves around the $\mathbf{x}$ axis by an angle α and the $(\mathbf{i},\mathbf{j},\mathbf{k})$ itself rotates around the $\mathbf{y}$ axis by an angle β. Also, $\mathbf{j}=\mathbf{y}$ and $\mathbf{i}=\mathbf{j}\times\mathbf{k}$. These axes will be useful later in the analysis. The *U-joint* twist and wrench systems are thus defined by:

$$\begin{aligned}\mathscr{V} &= \{\zeta_{\mathbf{0}}(\mathbf{x}),\zeta_{\mathbf{0}}(\mathbf{y})\},\\ \mathscr{T} &= \{\xi_{\mathbf{0}}(\mathbf{i}),\xi_{\mathbf{0}}(\mathbf{j}),\xi_{\mathbf{0}}(\mathbf{k}),\xi_{\infty}(\mathbf{z})\}.\end{aligned} \tag{1}$$

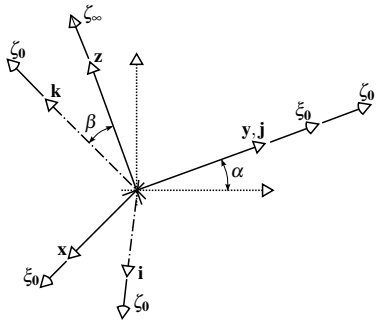

FIGURE 3. U-JOINT GEOMETRY

Computation of the mobility of Platforms A and B

To obtain the mobilities of the mechanism, only platforms A and B joined by the legs 1, 2 and 3 are first considered. It is possible to decompose this subsystem in two platforms linked by a triangular based prism (*TBP*) as shown in Figure 4. Using this figure, it can be shown that the instantaneous twist and wrench system of the *TBP* (at the left-hand side of Figure 4) is:

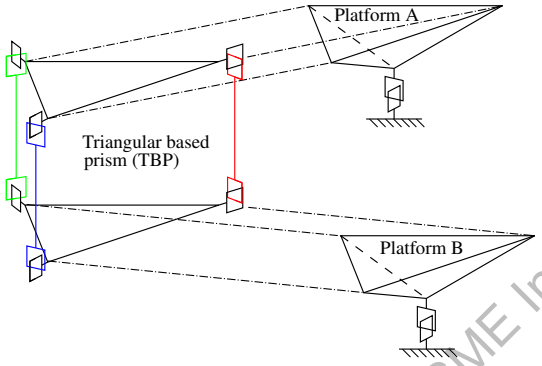

FIGURE 4. TRIANGULAR BASED PRISM DEFINITION

$$\mathcal{W}^{TBP} = \mathcal{T}^{TBP^\perp} = (\mathcal{T}^{TBP,1} \cup \mathcal{T}^{TBP,2} \cup \mathcal{T}^{TBP,3})^\perp. \quad (2)$$

Where $\mathcal{T}^{TBP,i} = \mathcal{W}^{TBP,i^\perp}$ for $i = 1,2,3$ are the wrench systems of every leg of the *TBP*. The geometry of these legs are illustrated in Figure 5.

Considering this geometry, one has:

$$\mathcal{W}^{TBP,i} = \left\{ \xi_0(\mathbf{x}_1^{TBP,i}), \xi_0(\mathbf{y}_1^{TBP,i}), \xi_0(\mathbf{x}_2^{TBP,i}), \xi_0(\mathbf{y}_2^{TBP,i}) \right\}, \quad (3a)$$

$$\mathcal{T}^{TBP,i} = \mathcal{W}^{TBP,i^\perp} = \left\{ \zeta_0(\mathbf{k}_1^{TBP,i}), \zeta_\infty(\mathbf{z}_1^{TBP,i}) \right\}. \quad (3b)$$

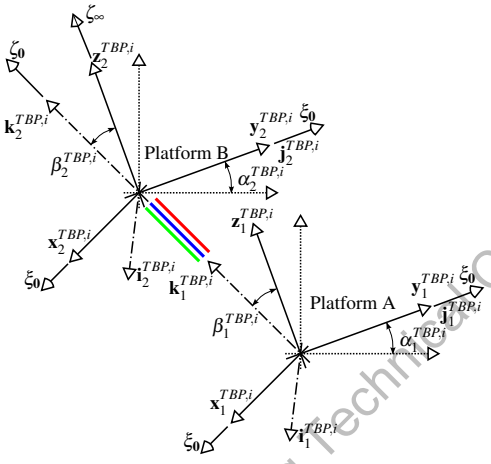

FIGURE 5. LEG i OF THE *TBP*

Equation (3b) has however some conditions. Indeed, the planes $(\mathbf{x}_1^{TBP,i}, \mathbf{y}_1^{TBP,i})$ and $(\mathbf{x}_2^{TBP,i}, \mathbf{y}_2^{TBP,i})$ must be parallel. With this, $\mathbf{x}_1^{TBP,i} \parallel \mathbf{x}_2^{TBP,i}$ and $\mathbf{k}_1^{TBP,i} \parallel \mathbf{k}_1^{TBP,j}\ \forall i \neq j$. Thus, condition must be met to make sure these planes are indeed parallel: namely, the three platforms and the three legs are identical. The wrench system is then given by:

$$\mathcal{T}^{TBP} = \left\{ \begin{array}{l} \zeta_0(\mathbf{k}_1^{TBP,1}), \zeta_0(\mathbf{k}_1^{TBP,2}), \zeta_0(\mathbf{k}_1^{TBP,3}), \\ \zeta_\infty(\mathbf{z}_1^{TBP,1}), \zeta_\infty(\mathbf{z}_1^{TBP,2}), \zeta_\infty(\mathbf{z}_1^{TBP,3}) \end{array} \right\} \quad (4)$$

and the twist system of the *TBP* is therefore:

$$\mathcal{W}^{TBP} = \left\{ \xi_\infty(\mathbf{i}^{TBP}), \xi_\infty(\mathbf{j}^{TBP}) \right\} \quad (5)$$

with $\mathbf{j}^{TBP} = \mathbf{y}_1^{TBP,1}$, $\mathbf{k}^{TBP} \parallel \mathbf{k}_1^{TBP,i}$ and $\mathbf{i}^{TBP} = \mathbf{j}^{TBP} \times \mathbf{k}^{TBP}$. Note that $\mathbf{j}^{TBP}$ is used from the first link but it could had been taken from any of the three links.

The twist system of the platforms is illustrated by Figure 6 where $\lambda = A$ or B.

Using the parameters defined in Figure 6, one has:

$$\mathcal{W}^{\lambda} = \left\{ \xi_0(\mathbf{x}^{\lambda}), \xi_0(\mathbf{y}^{\lambda}) \right\}, \quad (6a)$$

$$\mathcal{T}^{\lambda} = \left\{ \zeta_0(\mathbf{x}^{\lambda}), \zeta_0(\mathbf{y}^{\lambda}), \zeta_0(\mathbf{z}^{\lambda}), \zeta_\infty(\mathbf{k}^{\lambda}) \right\}. \quad (6b)$$

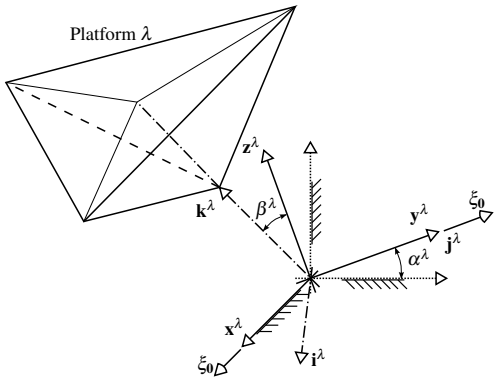

FIGURE 6. PLATFORM MOBILITY PARAMETERS

The twist and wrench systems of platform B can be calculated as:

$$\mathscr{W}^B = \mathscr{T}^{B\perp} = (\mathscr{T}^{B,1} \cup \mathscr{T}^{B,2})^\perp, \tag{7a}$$

$$\mathscr{T}^{B,1} = \mathscr{W}^{B,1\perp} = (\mathscr{W}^A \cup \mathscr{W}^{TBP})^\perp, \tag{7b}$$

$$\mathscr{T}^{B,2} = \mathscr{T}^B. \tag{7c}$$

Since the position of $\mathbf{k}^{TBP}$ is not constrained, it is possible to place it in order to coincide with the origin of $(\mathbf{x}^A, \mathbf{y}^A, \mathbf{z}^A)$. Therefore, $\mathbf{k}^{TBP}$ can be coplanar to $\mathbf{x}^A$, $\mathbf{y}^A$ and $\mathbf{z}^A$. Thus, one obtains:

$$\mathscr{W}^{B,1} = \left\{\xi_0(\mathbf{x}^A), \xi_0(\mathbf{y}^A), \xi_\infty(\mathbf{i}^{TBP}), \xi_\infty(\mathbf{j}^{TBP})\right\}, \tag{8a}$$

$$\mathscr{T}^{B,1} = \left\{\zeta_0(\mathbf{k}^{TBP}), \zeta_\infty(\mathbf{z}^A)\right\}, \tag{8b}$$

with also:

$$\mathscr{W}^{B,2} = \left\{\xi_0(\mathbf{x}^B), \xi_0(\mathbf{y}^B)\right\}, \tag{9a}$$

$$\mathscr{T}^{B,2} = \left\{\zeta_0(\mathbf{i}^B), \zeta_0(\mathbf{j}^B), \zeta_0(\mathbf{k}^B), \zeta_\infty(\mathbf{z}^B)\right\}. \tag{9b}$$

It can be observed that because the two platforms are identical and because $\mathbf{k}^{TBP}$ is aligned with the origin of $(\mathbf{x}^A, \mathbf{y}^A, \mathbf{z}^A)$, $\mathbf{k}^{TBP}$ will also be aligned with the origin of $(\mathbf{x}^B, \mathbf{y}^B, \mathbf{z}^B)$ and therefore, be coplanar with $\mathbf{x}^B$, $\mathbf{y}^B$ and $\mathbf{z}^B$. Thus, the twist and wrench systems of platform B are given by:

$$\mathscr{T}^B = \left\{\zeta_0(\mathbf{i}^B), \zeta_0(\mathbf{j}^B), \zeta_0(\mathbf{k}^B), \zeta_\infty(\mathbf{z}^B), \zeta_0(\mathbf{k}^{TBP}), \zeta_\infty(\mathbf{z}^A)\right\}, \tag{10a}$$

$$\mathscr{W}^B = \left\{\xi_0(\mathbf{x}^B), \xi_0(\mathbf{y}^B)\right\}. \tag{10b}$$

The first conclusion that can be drawn by this analysis is that the subsystem A-*TBP*-B can actually moves. Secondly, the two platforms keep the same orientation, i.e. $\alpha_B = \alpha_A$ and $\beta_B = \beta_A$. Indeed, since the *TBP* doesn't allow rotations (no ξ_0 possible) the two platforms stay be parallel.

Computation of the mobility of Platform C

The first step to establish the mobility of platform C is to find the individual twist system of every legs (1, 2 and 3). Indeed, platform C can be considered as the mobile platform of a parallel mechanism with three legs (legs 1, 2 and 3) composed by *U-joints*. The geometry of an arbitrary leg of the mechanism is given in Figure 7.

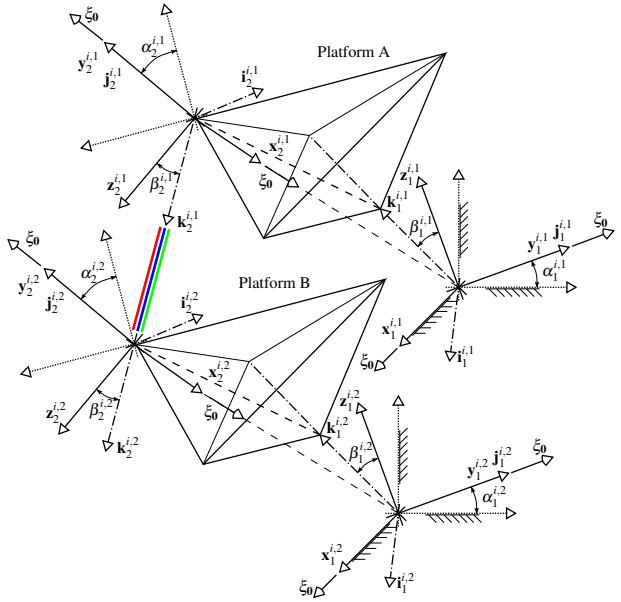

FIGURE 7. LEG GEOMETRY DEFINITION

From Figure 7, one has:

$$\mathscr{W}^i = \mathscr{T}^{i\perp} = \left(\mathscr{T}^{i,1} \cup \mathscr{T}^{i,2}\right)^\perp = \left(\mathscr{W}^{i,1\perp} \cup \mathscr{W}^{i,2\perp}\right)^\perp, \quad (11a)$$

$$\mathscr{W}^{i,j} = \left\{\xi_{\mathbf{0}}(\mathbf{x}_1^{i,j}), \xi_{\mathbf{0}}(\mathbf{y}_1^{i,j}), \xi_{\mathbf{0}}(\mathbf{x}_2^{i,j}), \xi_{\mathbf{0}}(\mathbf{y}_2^{i,j})\right\}, \quad (11b)$$

$$\mathscr{T}^{i,j} = \left\{\zeta_{\mathbf{0}}(\mathbf{x}_2^{i,j})\right\}, \quad (11c)$$

$$\mathscr{T}^{i} = \left\{\zeta_{\mathbf{0}}(\mathbf{x}_2^{i,1}), \zeta_{\mathbf{0}}(\mathbf{x}_2^{i,2})\right\}. \quad (11d)$$

Knowing, from the previous analysis, that $\mathbf{x}_2^{i,1} \parallel \mathbf{x}_2^{i,2}$, it can be asserted that leg i cannot leave the plane constituted by the two vectors $\mathbf{x}_2^{i,1}$ and $\mathbf{x}_2^{i,2}$. Therefore, as with planar screws, two supplementaries wrenches can be added: $\zeta_\infty(\mathbf{k}_2^{i,1})$ and $\zeta_\infty(\mathbf{x}_2^{i,1})$. As a result:

$$\mathscr{T}^{i} = \left\{\zeta_{\mathbf{0}}(\mathbf{x}_2^{i,1}), \zeta_{\mathbf{0}}(\mathbf{x}_2^{i,2}), \zeta_\infty(\mathbf{k}_2^{i,1}), \zeta_\infty(\mathbf{x}_2^{i,1})\right\}, \quad (12a)$$

$$\mathscr{W}^{i} = \left\{\xi_\infty(\mathbf{k}_2^{i,1}), \xi_\infty(\mathbf{j}_2^{i,2})\right\}. \quad (12b)$$

Once the twist and wrench systems of the links have been found, it is possible to add a *U-joint* and connect it to platform C, as illustrated in Figure 8.

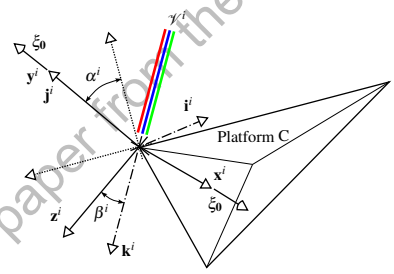

FIGURE 8. PLATFORM C GEOMETRY

From this, the wrench system of every leg connected to platform C is described by:

$$\mathscr{T}^{C,i} = \mathscr{W}^{C,i\perp} = \left(\mathscr{W}^i \cup \left\{\xi_{\mathbf{0}}(\mathbf{y}^{C,i}), \xi_{\mathbf{0}}(\mathbf{x}^{C,i})\right\}\right)^\perp, \quad (13a)$$

$$\mathscr{W}^{C,i} = \left\{\xi_\infty(\mathbf{k}_2^{i,1}), \xi_\infty(\mathbf{j}_2^{i,2}), \xi_{\mathbf{0}}(\mathbf{y}^{C,i}), \xi_{\mathbf{0}}(\mathbf{x}^{C,i})\right\}, \quad (13b)$$

$$\mathscr{T}^{C,i} = \left\{\zeta_{\mathbf{0}}(\mathbf{x}^{C,i}), \zeta_\infty(\mathbf{k}^{C,i})\right\}. \quad (13c)$$

Finally, the twist and wrench systems of platform C are thus defined by:

$$\mathscr{W}^{C} = \left(\mathscr{T}^{C}\right)^\perp = \left(\mathscr{T}^{C_1} \cup \mathscr{T}^{C_2} \cup \mathscr{T}^{C_3}\right)^\perp, \quad (14a)$$

$$\mathscr{T}^{C} = \left\{\begin{array}{l}\zeta_{\mathbf{0}}(\mathbf{x}^{C,1}), \zeta_{\mathbf{0}}(\mathbf{x}^{C,2}), \zeta_{\mathbf{0}}(\mathbf{x}^{C,3}),\\ \zeta_\infty(\mathbf{k}^{C,1}), \zeta_\infty(\mathbf{k}^{C,2}), \zeta_\infty(\mathbf{k}^{C,3})\end{array}\right\}, \quad (14b)$$

$$\mathscr{W}^{C} = \left\{\xi_{\mathbf{0}}(\mathbf{x}^{C}), \xi_{\mathbf{0}}(\mathbf{y}^{C})\right\}, \quad (14c)$$

where the axis $\mathbf{x}^C$ and $\mathbf{y}^C$ intersect the axis $\mathbf{x}^{C,i}$ and are perpendicular to the axis $\mathbf{k}^{C,i}$. These systems are represented in Figure 9.

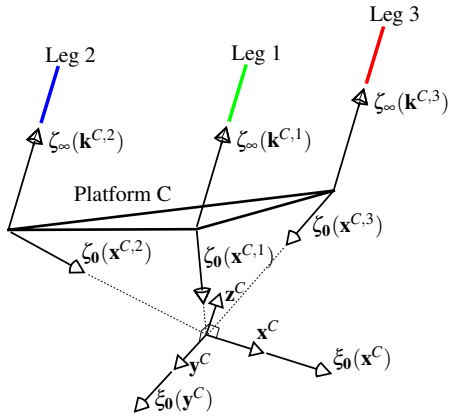

FIGURE 9. WRENCH AND TWIST SYSTEMS OF PLATFORM C

From this, it is possible to conclude that platform C has the same mobility than the two other platforms. Furthermore, since platforms B and C are connected by a *TBP*, as platforms A and B, it is possible to conclude that $\alpha_C = \alpha_B = \alpha_A$ and $\beta_C = \beta_B = \beta_A$. Thus from now on, these angles will simply be referred to as α and β.

Actuation / passive element locations

Now that the twist and wrench systems of the whole system have been determined, the addition of actuators (or passive elements for a RCC) is required. One way to achieve this is to install linear actuators between corners of the platform B and the base of platform A as shown in Figure 10. These actuators could be either pneumatic cylinder or simply springs. The actuators axes will be respectively referred to as $\mathbf{Ac_1}$ and $\mathbf{Ac_2}$.

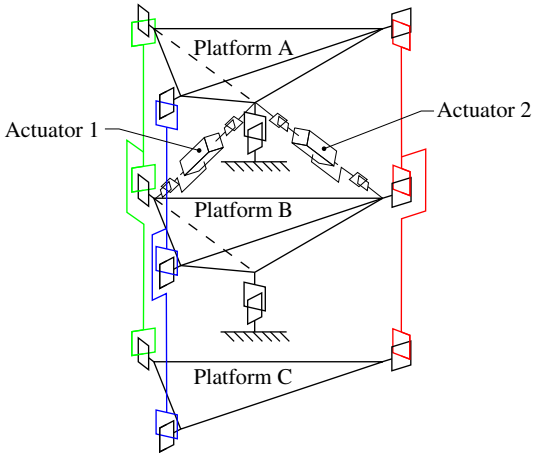

FIGURE 10. ACTUATORS LOCATIONS

The twist and wrench systems of platform B become:

$$\mathscr{W} = \mathscr{T}^{\perp} = \left(\mathscr{T}^{B} \cup \mathscr{T}^{Ac1} \cup \mathscr{T}^{Ac2}\right)^{\perp}, \tag{15a}$$

$$\mathscr{T}^{Ac_i} = \{\zeta_0(\mathbf{Ac_i})\}. \tag{15b}$$

Using Equations (6), one has:

$$\mathscr{T} = \left\{\zeta_0(\mathbf{x}^B), \zeta_0(\mathbf{y}^B), \zeta_0(\mathbf{z}^B), \zeta_\infty(\mathbf{k}^B), \zeta_0(\mathbf{Ac_1}), \zeta_0(\mathbf{Ac_2})\right\}, \tag{16a}$$

$$\mathscr{W} = \{\}, \tag{16b}$$

because it is not possible to find an axis perpendicular, parallel or intersecting $\mathbf{x}^B$, $\mathbf{y}^B$, $\mathbf{z}^B$, $\mathbf{Ac_1}$ and $\mathbf{Ac_1}$. Figure 11 illustrates the screws that are applied on platform B. In this case, the addition of these two actuators locks platform B and since $\alpha_C = \alpha_B = \alpha_A$ and $\beta_C = \beta_B = \beta_A$, the mobility of the whole system.

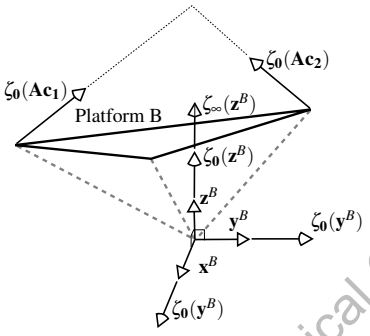

FIGURE 11. WRENCHES OF PLATFORM B

Velocity Relationship

As shown in the previous Sections, platform B can be controlled by two actuators. Therefore, there is a relationship between the two *DOF* (α and β) and the two actuated variables (δ_1 and δ_2). In fact, the relationship between the time derivatives $\left[\dot{\alpha}, \dot{\beta}\right]^{\top}$ and $\left[\dot{\delta}_1, \dot{\delta}_2\right]^{\top}$ needs to be obtained. For this, let us consider platform B with its three legs: the two actuators (presented in Figure 12) and the *U-joint* to the ground (Figure 6).

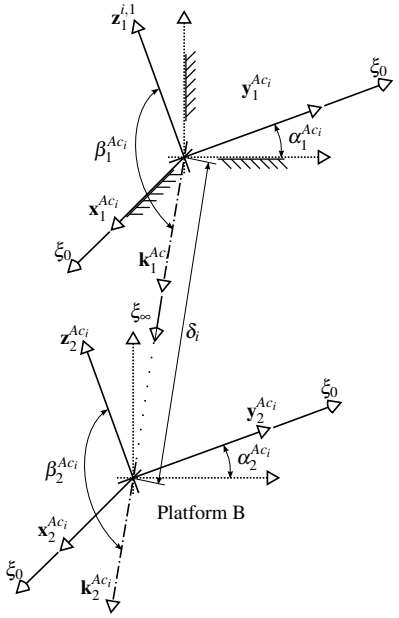

FIGURE 12. ACTUATION DEFINITION

The velocity equation of platform B is given by:

$$
\begin{aligned}
\xi &= \dot{\alpha}_1^{Ac_1}\xi_0(\mathbf{x}_1^{Ac_1}) + \dot{\beta}_1^{Ac_1}\xi_0(\mathbf{y}_1^{Ac_1}) + \dot{\delta}_1\xi_\infty(\mathbf{Ac_1}) + \cdots \\
&\quad \dot{\alpha}_2^{Ac_1}\xi_0(\mathbf{x}_2^{Ac_1}) + \dot{\beta}_2^{Ac_1}\xi_0(\mathbf{y}_2^{Ac_1}) \\
\xi &= \dot{\alpha}_1^{Ac_2}\xi_0(\mathbf{x}_1^{Ac_2}) + \dot{\beta}_1^{Ac_2}\xi_0(\mathbf{y}_1^{Ac_2}) + \dot{\delta}_2\xi_\infty(\mathbf{Ac_2}) + \cdots \\
&\quad \dot{\alpha}_2^{Ac_2}\xi_0(\mathbf{x}_2^{Ac_2}) + \dot{\beta}_2^{Ac_2}\xi_0(\mathbf{y}_2^{Ac_2}) \\
\xi &= \dot{\alpha}^{B}\xi_0(\mathbf{x}^{B}) + \dot{\beta}^{B}\xi_0(\mathbf{y}^{B}).
\end{aligned}
\tag{17}
$$

Now, knowing that the wrench systems $\{\zeta_0(\mathbf{Ac_1})\}$, $\{\zeta_0(\mathbf{Ac_2})\}$ and $\left\{\zeta_0(\mathbf{x}^B), \zeta_0(\mathbf{y}^B), \zeta_0(\mathbf{z}^B), \zeta_\infty(\mathbf{k}^B)\right\}$ are respectively reciprocal to the twist systems of every legs (except for the actuated joints), one can write:

$$
\begin{bmatrix} \zeta_0(\mathbf{Ac_1})\circ \\ \zeta_0(\mathbf{Ac_2})\circ \end{bmatrix} \xi = \begin{bmatrix} \zeta_0(\mathbf{Ac_1})\circ\xi_\infty(\mathbf{Ac_1}) & 0 \\ 0 & \zeta_0(\mathbf{Ac_2})\circ\xi_\infty(\mathbf{Ac_2}) \end{bmatrix} \begin{bmatrix} \dot{\delta}_1 \\ \dot{\delta}_2 \end{bmatrix}, \tag{18}
$$

which can be rewritten as:

$$
\mathbf{A}\xi = \mathbf{B}\dot{\delta}, \tag{19}
$$

with

$$
\xi = [\omega_x, \omega_y]^\top, \tag{20}
$$

where $\mathbf{A}$ and $\mathbf{B}$ are respectively the parallel and serial Jacobian matrices of the mechanism. To evaluate them, the screws have to be expressed in the same global coordinates. Let a global cartesian frame $(\mathbf{x}, \mathbf{y}, \mathbf{z})$ be centered at the origin of platform B and the axis $\mathbf{z}$ aligned with the origin of platform A and the center of rotation of platform C. The Jacobian matrices are then:

$$
\mathbf{A} = \begin{bmatrix} A_{11} & A_{12} \\ A_{21} & A_{22} \end{bmatrix} \tag{21}
$$

and

$$
\mathbf{B} = \begin{bmatrix} B_{11} & 0 \\ 0 & B_{22} \end{bmatrix}, \tag{22}
$$

with:

$$
\begin{aligned}
A_{11} &= S_\alpha \,\mathrm{dz}\left(C_\beta h - S_\beta b\right) \\
A_{12} &= \mathrm{dz}\left(C_\beta b + S_\beta h\right) \\
A_{21} &= \mathrm{dz}\left(C_\beta S_\alpha h - \frac{\sqrt{3}}{2} C_\alpha b + \frac{1}{2} S_\alpha S_\beta b\right) \\
A_{22} &= -\mathrm{dz}\left(\frac{1}{2} C_\beta b - S_\beta h\right) \\
B_{11} &= \left(\mathrm{dz} - C_\alpha\left(C_\beta h - S_\beta b\right)\right)^2 + \cdots \\
&\quad \left(C_\beta b + S_\beta h\right)^2 + {S_\alpha}^2\left(C_\beta h - S_\beta b\right)^2 \\
B_{22} &= \left(C_\alpha C_\beta h - \mathrm{dz} + \frac{1}{2} C_\alpha S_\beta b + \frac{\sqrt{3}}{2} S_\alpha b\right)^2 + \cdots \\
&\quad \left(\frac{1}{2} C_\beta b - S_\beta h\right)^2 + \left(C_\beta S_\alpha h - \frac{\sqrt{3}}{2} C_\alpha b + \frac{1}{2} S_\alpha S_\beta b\right)^2,
\end{aligned}
\tag{23}
$$

where d_z, b and h are geometric variables defined in Figure13.

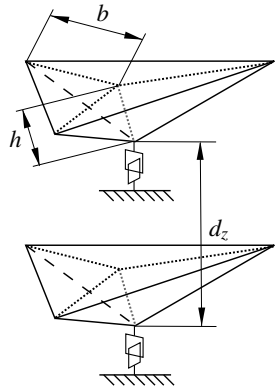

FIGURE 13. GEOMETRIC VARIABLES

OPTIMIZATION

Now that the kinematic of the mechanism has been studied and that the desired twist and wrench systems have been established, the next step is to optimize its dimensions. Since many parameters are already fixed by assumptions, the only remaining variable are given in Figure 13.

The first criterion chosen for the optimization is the conditioning of the Global Jacobian matrix $\mathbf{J} = \mathbf{A}^{-1}\mathbf{B}$. Indeed, a minimal condition number helps to reduce the required actuator velocities. With this in mind, one can define a proper performance function. As the Jacobian matrix depends on the orientation of the platforms, each angle (α and β) will be discretized the condition number will be evaluated for $(\alpha_i, \beta_j)\ \forall i \in 1,2,...,n, j \in 1,2,...,m$. The performance function is given:

$$S_1 = \max(C) + \mathrm{mean}(C). \tag{24}$$

However, this relation does not lead to a unique solution. Indeed, it is easy to see that a scaled up version of the mechanism would perform identically to the original. To solve this issue, let us consider two additional parameters p_b and p_h defined by:

$$p_b = \frac{b}{d_z}, \tag{25a}$$

$$p_h = \frac{h}{d_z}, \tag{25b}$$

$$d_z > 0. \tag{25c}$$

A second criterion that can be used based on the latter is the compactness of the mechanism. Indeed, an optimal mechanism must be the most compact possible but still be capable of offering the desired mobility. Therefore, the volume of the tetrahedron composed of the platforms will also be consider for the optimization. This volume is defined by equation:

$$V = \frac{3\sqrt{3}}{2} b^2 h. \tag{26}$$

Then, the parameters defined in Equation (25) can be used to get rid of the scaling issue. A second performance index can then be:

$$S_2 = P_b^2 P_h. \tag{27}$$

Finally, the global optimization function $S = S_1 + S_2$ is used which reaches its minimum value when the maximal condition number, the average condition number and the normalized volume are minimal.

Results

Using a genetic algorithm from a numerical software package, the optimal values are obtained as presented in Table 1.

TABLE 1. OPTIMIZATION RESULTS

Population size	P_b	P_h	S
5	0.523	0.221	4.6307
10	0.516	0.200	4.6304
20	0.516	0.200	4.6302
40	0.513	0.200	4.6301
80	0.513	0.200	4.6300

It is possible to see that when the population size increases, the solution tends to $P_b = 0.513$ and $P_h = 0.200$. These parameters will be used for the final design of the mechanism. Note that P_h is limited to a minimal value of 0.2 in order to ensure that the *SCG* can be properly mounted in the mechanism.

COMPLIANT VERSION

The final step of this paper is to develop a compliant version of the mechanism previously studied. The motivation of this conversion is to remove the actuators and use passive elements instead. In the previous Sections, it was mentioned that these actuators could simply be linear springs, yet these "actuators" only store energy the work done during the rotation of platform C. Indeed, a typical disadvantage of compliant mechanisms is to store energy instead of transmitting it. However, in the case of shape adaptation this is irrelevant. Therefore, the approach will be to remove the actuators and transform the *U-joint* defined in Figure 1 into a fully compliant joint with the same properties.

Compliant U-joint

An approach to design a compliant U-joint would be to use the design described in [20], illustrated in Figure 14.

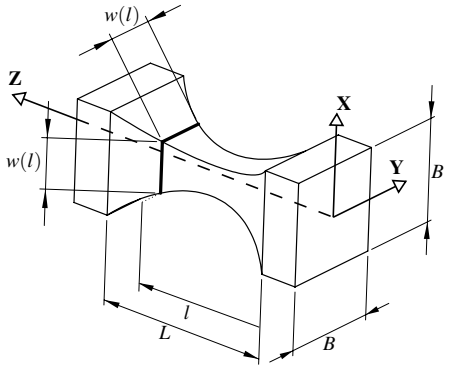

FIGURE 14. COMPLIANT U-JOINT

This compliant design has a low stiffness in rotation around **x** and **y** and low compliance in other directions. This compliant joint can be described by a pseudo-rigid body model and it is possible to compute the equivalent stiffness of the model by equation:

$$K_{M_\theta} = \frac{EI}{L}, \tag{28}$$

where K_{M_θ} is the stiffness of the decoupled rotation, I is the second moment of area, J is the second moment of area in torsion and E is the Young modulus.

Global rigidity

It is finally possible to evaluate the global stiffness of the mechanism using a virtual work approach. Using the definition of a *U-joint* in Figure 1, one has:

$$Tj_{i_x} = K_{M\theta}\Delta\alpha, \tag{29}$$

and

$$Tj_{i_y} = K_{M\theta}\Delta\beta. \tag{30}$$

Here i identifies the joint (from 1 to 11). The virtual work of the system can then be written as:

$$\delta W = \delta W_{in} + \sum_{i=1}^{11} \delta W j_i = 0, \tag{31}$$

where W_{in} is the work done by the torques at the mobile platform and Wj_i is the work done by the passive elements in the joints. The combination of Equations (29), (30) and (31) leads to:

$$T_x\delta\alpha + T_y\delta\beta = \sum_{i=1}^{11} \Delta\alpha_i K_{M\theta}\delta\alpha_i + \sum_{i=1}^{11} \Delta\beta_i K_{M\theta}\delta\beta_i \tag{32}$$

As it had been shown in the previous Sections that the legs always stay parallel to the axis defined by the centers of rotation of platforms A and B, and because the orientation of the platforms are the same, the bending angles of every joints are also the same. Therefore, $\alpha_i = \alpha\ \forall i = 1,2,\cdots,11$ and $\beta_i = \beta\ \forall i = 1,2,\cdots,11$. Finally, Equation (32) becomes:

$$(T_x - 11\Delta\alpha K_{M\theta})\delta\alpha + (T_y - 11\Delta\beta K_{M\theta})\delta\beta = 0 \tag{33}$$

The global stiffness of the mechanism is thus defined by:

$$K_{eq} = 11K_{M\theta}, \tag{34}$$

with:

$$T_x = \Delta\alpha K_{eq}, \tag{35a}$$

$$T_y = \Delta\beta K_{eq}. \tag{35b}$$

Simulation and results

In order to verify the mobility of the mechanism as well as the choice of the compliant joint, a model has been created in a CAD software *CATIA V5*. The dimensions used for this model are given in Table 2.

TABLE 2. GEOMETRIC PARAMETERS

Dimension	Value (mm)	Equation
h	25.1	n/a
b	64.381	$\frac{P_b}{P_h}h$
dz	125.5	$\frac{1}{P_h}h$
L	10	n/a
B	10	n/a
$w(l)$	n/a	$\frac{3B}{L^2}\left(l-\frac{L}{2}\right)^2+\frac{1}{4}B$

Using *Finite Element Analysis* (*FEA*) module, it is possible apply a torque to the *SCG*. This loading represents the *SCG* force into a non parallel surface as shown in Figure 1. The result of this is presented in Figure 15. It is possible to see that the rotation is indeed obtained around the center of the suction plate as required.

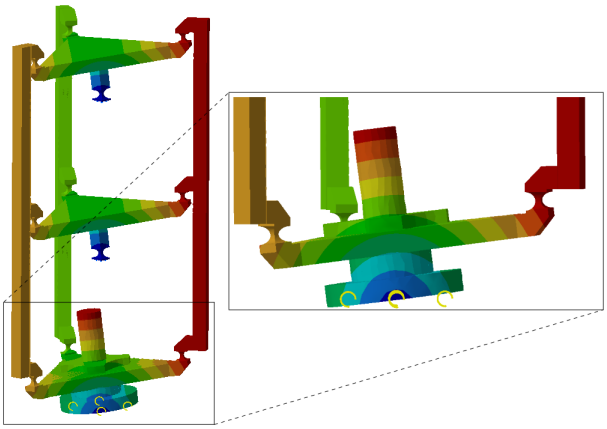

FIGURE 15. SIMULATION RESULTS - DISPLACEMENT GRADIENT

CONCLUSION

To conclude, this paper has demonstrated, using screw theory, that the introduced mechanism allows platform C to have the same motion as ifif it was connected with a *U-joint* to the ground (such as platforms A and B). Then, the optimization, using an genetic algorithm, allowed to obtain geometrical parameters to ensure a minimal conditioning of the Jacobian Matrix. Finally, *FEA* of the design has shown that the mechanism behaves appropriately.

ACKNOWLEDGMENT

The authors acknowledge the support of CTT Group in this project.

REFERENCES

[1] Angerer, A., Ehinger, C., Hoffmann, A., Reif, W., Reinhart, G., and Strasser, G., 2010. "Automated cutting and handling of carbon fiber fabrics in aerospace industries". In 2010 IEEE International Conference on Automation Science and Engineering, CASE 2010, August 21, 2010 - August 24, 2010, IEEE Computer Society, pp. 861–866.

[2] Gao, Z., and Reifsnider, K. L., 1993. "Micromechanics of tensile strength in composite systems". In 4th Symposium on Composite Materials, May 6, 1991 - May 7, 1991, Publ by ASTM, pp. 453–470.

[3] Subramanian, S., Reifsnider, K. L., and Stinchcomb, W. W., 1995. "Tensile strength of unidirectional composites: The role of efficiency and strength of fiber-matrix interface". *Journal of Composites Technology and Research,* ***17***(4), pp. 289–300.

[4] Apmann, H., 2008. "Automatic handling of cfrp-material for frame and stringer production". In Aerospace Manufacturing and Automated Fastening Conference and Exhibition, September 16, 2008 - September 18, 2008, SAE International.

[5] Apmann, H., 2009. "Automatic handling of dry carbon fabrics and prepregs". In 17th International Conference on Composite Materials, ICCM-17, July 27, 2009 - July 31, 2009, International Committee on Composite Materials, p. Office of Naval Research Science and Technology (ONR); INSTRON; ELSEVIER; Vestas; AIRBUS.

[6] Apmann, H., Hemmen, A., and Herkt, M., 2012. "Automatic handling of carbon fiber preforms for cfrp parts in aerospace". In SAE 2012 Aerospace Manufacturing and Automated Fastening Conference and Exhibition, AMAF 2012, September 18, 2012 - September 20, 2012, Vol. 6, SAE International.

[7] Kordi, M. T., Husing, M., and Corves, B., 2007. "Development of a multifunctional robot end-effector system for automated manufacture of textile preforms". In 2007 IEEE/ASME International Conference on Advanced Intelligent Mechatronics, AIM, September 4, 2007 - September 7, 2007, Institute of Electrical and Electronics Engineers Inc., p. IEEE Robotics and Automation Society; IEEE Industrial Electronics Society; ASME Dynamic Systems and Control Division; ETH Zurich.

[8] Reinhart, G., and Straer, G., 2011. "Flexible gripping technology for the automated handling of limp technical textiles in composites industry". *Production Engineering,* ***5***(3), pp. 301–306.

[9] Tarsha, M., Husing, M., and Corves, B., 2007. "Robot end-effector for local fabric manipulation for automated manufacture of textile preforms". *VDI Berichte*(1980), pp. 341–352.

[10] Chestney, J. A., Zhang, Z., and Sarhadi, M., 1994. "Robotic handling of carbon fibre materials with electrostatic grippers". In European Conference on Robotics and Intelligent Systems, 22-25 Aug. 1994, Vol. vol.2, Univ. Bristol, pp. 695–707.

[11] Fleischer, J., Frster, F., and Crispieri, N. V., 2014. "Intelligent gripper technology for the handling of carbon fiber material". *Production Engineering,* ***8***(6), pp. 691–700.

[12] J., F., S., O., and F., F., 2013. "Gripping technology for carbon fibre material.". In CIRP International conference on competitive manufacturing.

[13] Molfino, R., Zoppi, M., Cepolina, F., Yousef, J., and Cepolina, E. E., 2014. "Handling carbon fiber fabric in agile manufacturing cells". *WSEAS Transactions on Circuits and Systems,* ***13***, pp. 253–261.

[14] Watson, P. C., 1977. "Remote center compliance system and its application to high speed robot assemblies". *Technical Paper - Society of Manufacturing Engineers. AD*.

[15] Whitney, D. E., and Nevins, J. L., 1979. "What is the remote center compliance (rcc) and what can it do?". *Water*

Resources and Environmental Engineering Research Report (State University of New York at Buffalo, Department of Civil Engineering), pp. 135–152.

[16] Lane, J. D., 1979. "Applications of the remote center compliance device to assembly operations". *Technical Paper - Society of Manufacturing Engineers. MS*(79-872).

[17] Jain, R. K., Majumder, S., and Dutta, A., 2013. "Active 4 dof based rcc wrist using segmented ipmcs for robotic peg-in-hole assembly". In 52nd Annual Conference of the Society of Instrument and Control Engineers of Japan (SICE 2013), 14-17 Sept. 2013, IEEE, pp. 2625–31.

[18] Qiao, H., Dalay, B. S., and Parkin, R. M., 1994. "Precise robotic chamferless peg-hole insertion operation without force feedback and remote centre compliance (rcc)". *Proceedings of the Institution of Mechanical Engineers, Part C (Journal of Mechanical Engineering Science),* ***208***(C2), pp. 89–104.

[19] Zhao, F., and Wu, P. S. Y., 1998. "Vrcc : a variable remote center compliance device". *Mechatronics,* ***8***(6), pp. 657–672.

[20] Lobontiu, N., and Garcia, E., 2003. "Two-axis flexure hinges with axially-collocated and symmetric notches". *Computers and Structures,* ***81***(13), pp. 1329–1341.

[21] Lai, L.-J., Gu, G.-Y., Zhou, H., and Zhu, L.-M., 2013. *Design and Analysis of a Spatial Remote Center of Compliance Mechanism*. Springer, pp. 385–396.

[22] Parlaktaş, V., and Tanık, E., 2014. "Single piece compliant spatial slider–crank mechanism". *Mechanism and Machine Theory,* ***81***(0), pp. 1–10.

[23] Trease, B. P., Moon, Y.-M., and Kota, S., 2004. "Design of large-displacement compliant joints". *Journal of Mechanical Design,* ***127***(4), pp. 788–798.

[24] Farhadi Machekposhti, D., Tolou, N., and Herder, J. L.", 2012.".

[25] Palmieri, G., Palpacelli, M. C., and Callegari, M., 2012. "Study of a fully compliant u-joint designed for minirobotics applications". *Journal of Mechanical Design, Transactions of the ASME,* ***134***(11).

[26] Tanik, E., and Parlaktas, V., 2012. "Compliant cardan universal joint". *Journal of Mechanical Design,* ***134***(2), p. 021011 (5 pp.).